International Journal of Nanomedicine

Dovepress
Taylor & Francis Group

Open Access Full Text Article

ORIGINAL RESEARCH

Adipose Tissue-Derived Extracellular Vesicles Loaded with miR-141-3p Regulate Obesity-Induced Insulin Resistance by Targeting Glycogen Synthesis and Gluconeogenesis

Zixian Wang[1,2,*], Tianyu Ma[3,*], Ge Bai[2], Qianchen Fang[2], Biqian Ou[2], Meng Chen[2], Pei Xu[2], Meng Tian[2], Anding Xu[1], Yi Ma[1,2]

[1]The First Affiliated Hospital, Jinan University, Guangzhou, Guangdong, 510630, People's Republic of China; [2]Department of Cellular Biology, Institute of Biomedicine, National Engineering Research Center of Genetic Medicine, Key Laboratory of Bioengineering Medicine of Guangdong Province, Jinan University, Guangzhou, Guangdong, 510632, People's Republic of China; [3]School of Medicine, Jinan University, Guangzhou, Guangdong, 510632, People's Republic of China

*These authors contributed equally to this work

Correspondence: Yi Ma; Anding Xu, The First Affiliated Hospital, Jinan University, Guangzhou, Guangdong, 510630, People's Republic of China, Email tmayi@jnu.edu.cn; tlil@jnu.edu.cn

Purpose: Insulin resistance, a hallmark feature of type 2 diabetes and cardiovascular diseases, is critically influenced by liver-adipose tissue crosstalk, offering a novel therapeutic strategy for its management. Emerging evidence indicates that extracellular vesicles (EVs) secreted from adipose tissue serve as essential carriers of miRNA-mediated interorgan communication. This study aimed to investigate the regulatory effects of adipose tissue-derived EVs on obesity-induced hepatic insulin resistance and to elucidate the underlying molecular mechanisms by which EV-mediated signaling contributes to metabolic dysfunction.

Methods: EVs with miR-141-3p knockout or overexpression were constructed and administered to both in vitro cell models and in vivo mouse models to investigate the regulatory role and underlying mechanisms of miR-141-3p-mediated adipose tissue-derived EVs in obesity-induced hepatic insulin resistance.

Results: miR-141-3p is significantly upregulated in adipose tissue-derived EVs from high-fat diet (HFD)-fed mice, as well as in other obesity-related conditions. Furthermore, the knockdown of miR-141-3p in EVs from chow diet (CD-EVs) counteracted the effect in improving obesity-induced hepatic insulin resistance, whereas the overexpression of miR-141-3p in HFD-EVs improved hepatic insulin resistance. Mechanistically, EVs-derived miR-141-3p directly targets PTEN to promote PI3K/AKT signaling, thereby mediating hepatic glucose homeostasis through the regulation of hepatic gluconeogenesis and glycogen synthesis.

Conclusion: In summary, our results highlight the emerging role of miR-141-3p in mediating adipose tissue-derived EVs to alleviate obesity-induced hepatic insulin resistance, providing potential therapeutic targets for type 2 diabetes.

Keywords: insulin resistance, glycogen synthesis, gluconeogenesis, extracellular vesicles, miRNA, PTEN

Introduction

Insulin resistance is a significant factor in the development and progression of the vast majority of type 2 diabetes (T2D).[1] The liver plays a central role in systemic metabolic regulation, particularly in glucose metabolism and lipid metabolism, and aberrant hepatic insulin action is thought to be a major driver of insulin resistance.[2] The liver maintains glucose homeostasis through glycolysis (glucose consumption), glycogen synthesis (glucose storage), and gluconeogenesis (glucose release).[3] Under conditions of hepatic insulin resistance, the effect of insulin is impaired, resulting in decreased hepatic glycogen synthesis and increased gluconeogenesis, leading to persistent hepatic glucose output and postprandial hyperglycemia.[4,5]

Received: 12 December 2024
Accepted: 11 April 2025
Published: 3 May 2025

Obesity has emerged as a significant contributor to insulin resistance globally.[6] Obesity has become a widespread epidemic worldwide, resulting in a concurrent increase in the prevalence of T2D.[7] The abnormal accumulation of adipose tissue in various parts of the body is a key driver of insulin resistance (IR).[8] Previous studies have demonstrated that the liver plays a pivotal role in regulating the metabolism of other organs, including adipose tissue, through the secretion of FGF21, IGF1, or extracellular vesicles.[9–11] Adipose tissue, as a specialized endocrine organ, secretes a variety of cytokines, such as TNF-α, IL-6, adiponectin, and leptin, which influence the functions of other tissues.[12,13] The crosstalk between the liver, adipose tissue, and other tissues through specific bioactive factors is essential for maintaining metabolic homeostasis. However, there are few reports on the crosstalk between the liver and adipose tissue.

Emerging evidence has demonstrated that extracellular vesicles function as signaling vehicles for cell-cell communication, cell-tissue communication, and tissue-tissue communication.[14,15] Extracellular vesicles derived from diverse cell types facilitate intercellular communication by delivering bioactive molecules, including proteins, lipids, and RNAs (miRNAs, mRNAs, lncRNAs, and circRNAs), to neighboring and distant target cells and tissues.[16,17] Previous studies have demonstrated that extracellular vesicles play a critical role in modulating glucose and lipid metabolic homeostasis.[18,19] Among the key signaling molecules carried by EVs, miRNAs have emerged as pivotal regulators of glucose and lipid metabolism.[20]

miR-141-3p, a member of the miR-200 family, is widely involved in the progression and metastasis of various cancers.[21,22] Notably, miR-141-3p is associated with insulin resistance and type 2 diabetes,[23] however, research in this area remains relatively scarce. Additionally, previous studies have reported that phosphatase and tensin homolog (PTEN) may be a target of miR-141-3p.[24,25] The tumor suppressor PTEN, a protein and lipid phosphatase, antagonizes the phosphatidylinositol 3-kinase (PI3K) pathway and plays a pivotal regulatory role in insulin signaling.[26] As a negative regulator of the insulin signaling pathway, PTEN suppresses downstream signaling cascades to maintain metabolic homeostasis.[27,28] Our previous study preliminarily demonstrated that exosomes containing miR-141-3p obtained from lean adipose tissue can improve hepatic insulin resistance by targeting PTEN. Nonetheless, the precise molecular mechanism underlying its effect remains unclear.[29]

In our previous study, we demonstrated that EVs released from obese adipose tissue impair insulin sensitivity and glucose uptake in hepatocytes by transferring reduced miR-141-3p.[29] However, whether adipose tissue-derived EVs regulate obesity-induced hepatic insulin resistance through miR-141-3p and the underlying mechanisms remain unexplored. In this study, miR-141-3p knockout and overexpressing EVs were constructed to further investigate the potential regulatory role and molecular mechanisms of miR-141-3p-mediated adipose tissue-derived EVs in obesity-induced hepatic insulin resistance.

Materials and Methods

Animals and Treatments

Five-week-old male C57BL/6 mice were purchased from Beijing Huabengkang Biotechnology Co., Ltd (Beijing, China) and raised in a specific pathogen-free (SPF) environment. Five mice per cage were housed under controlled conditions with an ambient temperature of 20–25°C, a humidity of 45–55%, and a 12-hour light-dark schedule. All mice had ad libitum access to food and tap water during the entire protocol. After a 7-day acclimation period, the mice were randomly assigned to two groups and fed a normal chow diet (TP2330055AC; calories fat 10%, carbohydrate 75%, and protein 15%; Trophic Animal Feed High-tech Co., Ltd, China) or a high-fat diet (TP2330055A; calories fat 60%, carbohydrate 25%, and protein 15%; Trophic Animal Feed High-tech Co. Ltd, China) to produce diet-induced obesity model mice, as described previously.[30] During the experiment, the body weight and food intake of each group were recorded weekly. To investigate the effects of miRNAs on HFD-fed mice, HFD-fed mice were randomly divided into five groups and injected with 30 μg of adipose tissue EVs from different sources or modifications via the tail vein (twice per week) for 3 weeks. The animal study was conducted in accordance with the Guidelines for the Care and Use of Laboratory Animals of the Chinese Animal Welfare Committee, and the protocols were approved by the Animal Care Committee of Jinan University.

AML12 Cell and Model Establishment

Mouse hepatocytes (AML12 cells) were purchased from the Type Culture Collection of the Chinese Academy of Sciences (Shanghai, China), and cultured in 1:1 mixture DMEM/F12 (Gibco, US) supplemented with 10% fetal bovine serum (FBS; BI, South America), 1% Insulin–Transferrin–Selenium Solution (ITS; Sigma-Aldrich, USA), 40 ng/mL dexamethasone (Macklin, China) and 1% Penicillin Streptomycin (Gibco, USA). The cells were cultured at 37°C in a humidified atmosphere with 5% CO_2. In vitro cell experiments, cells were treated with 200 μM PA for 24 h to establish an obesity-induced insulin resistance model, and then treated with 10 μg/mL EVs from different sources in cell medium for another 48 h. Then, the cells were stimulated with insulin (100 nM) for 20 min at 37°C. Finally, the cells were collected for protein extraction, RNA isolation, and other experiments.

EVs Isolation and Identification

The adipose tissue was removed from 14-week-old normal mice or HFD-induced obese mice (WT; HFD) and rinsed in PBS three times. The adipose tissue was cut into 2 mm × 2 mm pieces. The minced tissue pieces were transferred to DMEM/F12 medium containing 10% exosome-free FBS (Thermo Fisher Scientific, USA), and the supernatant was collected after 12 h. Cultured supernatants were centrifuged at 500 ×g for 10 min and 2000 ×g for 10 min to remove cellular debris. The supernatant was centrifuged at 10,000 ×g for 40 min at 4°C, and then filtered through a 0.22-μm filter. The supernatants were concentrated using a protein concentrator with a 100-kDa cutoff (Millipore, USA). Finally, EVs were precipitated from the supernatant using an ExoQuick kit (System Biosciences, USA). EV protein concentration was quantified using a BCA Protein Assay kit (Thermo Fisher Scientific, USA). EVs were characterized by detecting exosomal markers (CD81, CD9, TSG101) and the negative control Calnexin via Western blotting. In addition, the samples were further analyzed by transmission electron microscopy (TEM) as previously described.[31]

EVs Labeling

To monitor EVs trafficking, extracellular vesicles were fluorescently labeled using the PKH26 Red Fluorescent Cell Linker Kit (Sigma-Aldrich, USA) according to the manufacturer's protocol. After PKH26 staining, unincorporated dye was removed from labeled EV preparations using Exosome Spin Columns (Invitrogen, USA). Subsequently, AML12 cells were incubated with 10 μg/mL PKH26-labeled EVs in an incubator at 37°C with 5% CO_2. After 6 h, the cells were fixed in 4% paraformaldehyde for 15 min and then stained with DAPI for 10 min. Fluorescence images were captured using a microscope (Olympus IX71, Japan).

Overexpression/Inhibition of miR-141-3p in EVs

The miR-141-3p mimic, miR-141-3p inhibitor, mimic negative control (mimic NC), and inhibitor negative control (inhibitor NC) were synthesized by GenePharma (Shanghai, China). These constructs were transfected into EVs with Lipofectamine RNAiMAX Reagent (Thermo Fisher Scientific, USA) according to the manufacturer's instructions. After incubation for 6 h at 37°C, an ExoQuick kit (System Biosciences, USA) was used to re-extract the EVs.

RNA Isolation and RT-qPCR

Total RNA was isolated from EVs, AML12 cells, or tissues using RNAiso Plus reagent (Takara, Japan) according to the manufacturer's instructions. RNA purity and concentration were measured using a NanoDrop 2000 Spectrophotometer (Thermo Fisher Scientific, USA). For RT-PCR, total RNA (2 μg) was reverse transcribed into cDNA using the ReverTra Ace qPCR RT Master Mix with genomic DNA remover (Toyobo, JAPAN). For miRNA RT-PCR, poly (A) addition to miRNA and reverse transcription were performed using miRNA First Strand cDNA Synthesis (Tailing Reaction; Sangon Biotech, China). Quantitative real-time PCR (qPCR) reactions were conducted using 2x SYBR Green qPCR Master Mix (Genstar, China). Relative expression levels of mRNA and miRNA were calculated by the $2^{-\Delta\Delta Ct}$ method, normalized to the internal reference genes RPLP0 and U6, respectively. Primer sequences are listed in Supplementary Table 1.

Western Blotting Assay

EVs, cells, and liver tissue were homogenized with RIPA buffer supplemented with protease and phosphatase inhibitors (Beyotime Biotechnology, China). After the protein concentration was determined using the BCA Protein Assay Kit (Thermo Fisher Scientific, USA), 30 μg of protein was separated on a 10% SDS–PAGE gel and then transferred onto a 0.2 μm polyvinylidene difluoride (PVDF) membrane (Pall Life Sciences, USA). Membranes were blocked with 5% BSA in TBST (Tris-buffered saline with Tween-20 solution) at room temperature for 1 h, followed by incubation with diluted primary antibodies at 4°C overnight. After five washes with TBST (10 minutes each), membranes were incubated with the appropriate horseradish peroxidase (HRP)-conjugated secondary antibodies for 1 h at room temperature. The chemiluminescence signals were examined using a SuperLumia ECL Plus HRP Substrate kit (Abbkine, China). Protein expression was normalized to GAPDH. The primary antibodies are listed in Supplementary Table 2.

Blood Glucose, Serum Insulin and HOMA-IR Index

After mice were fasted for 12 h, fasting blood glucose levels were measured using 5 μL tail vein blood applied to glucose test strips (Sinocare, China) and analyzed with a blood glucose meter (Sinocare, China), and serum insulin levels were measured using a mouse insulin ELISA kit (Excell Bio, China) according to the manufacturer's instructions. HOMA-IR was calculated as: [fasting blood glucose level (mmol/L)] × [fasting serum insulin level (μU/mL)]/22.5.[32]

Glucose Tolerance and Insulin Tolerance Tests

For the glucose tolerance test (GTT), mice were fasted for 12 hours and intraperitoneally injected with 2 g/kg glucose,[33] and the blood glucose concentration was determined from the tail vein at 0, 15, 30, 60, 90, and 120 min. For the insulin tolerance test (ITT), the mice were intraperitoneally injected with insulin at 0.4 IU/kg after fasting for 4 h. Blood glucose levels were measured at the indicated time points.

PAS Staining

For in vivo experiments, tissue samples were fixed in 4% paraformaldehyde for more than 24 h, followed by paraffin embedding. Then, the liver sections were sectioned at 5 μm and stained using a Periodic Acid-Schiff (PAS) kit (Bestbio, China) according to the manufacturer's instructions. In vitro experiments, IR-AML12 cells treated with EVs for 48 h were washed 3 times with PBS, fixed in 4% paraformaldehyde for 20 min, then washed with PBS 3 times. PAS staining was subsequently performed as described for in vivo samples.

Statistical Analysis

All data are expressed as the mean ± standard deviation (SD). Statistical analysis was performed using GraphPad Prism 8.0. The statistical significance of differences among groups was analyzed by one-way ANOVA, followed by the Newman-Keuls test. Comparisons between two groups were performed using a two-tailed Student's *t*-test. $p < 0.05$, $p < 0.01$ and $p < 0.001$ were considered statistically significant. Data are representative of at least three independent experiments.

Results

Adipose Tissue-Derived EVs Were Identified and Taken Up by Hepatocytes

The EVs extracted from the adipose tissue of the chow diet-fed and high-fat diet-fed mice were named CD-EVs and HFD-EVs, respectively (Figure 1A). To determine the quality of EVs, we analyzed the morphology by TEM and marker proteins of the EVs via Western blotting, respectively. TEM revealed that the particles isolated by centrifugation and exosome extraction kit methods contained abundant exosomes with a double-layered membrane structure and a diameter of 30–150 nm (Figure 1B). The extracellular particles released from adipose tissue expressed exosome markers (CD9, CD63, and TSG101) but not the exosome-negative marker Calnexin (Figure 1C). These data indicated that the main components of the harvested EVs were exosomes. To ascertain whether CD-EVs and HFD-EVs could be taken up by hepatocytes, PKH26-labeled EVs were co-cultured with

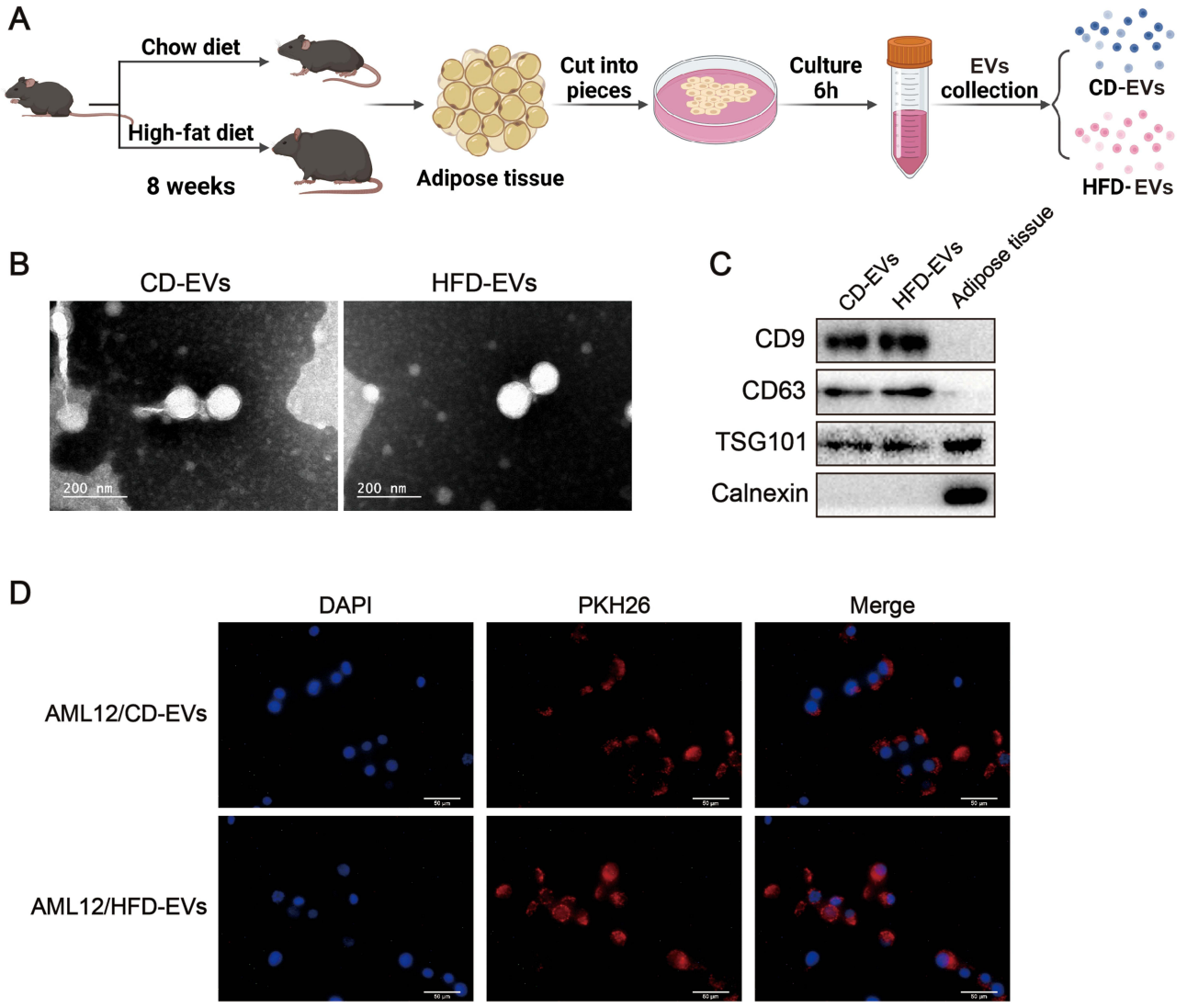

Figure 1 Characterization and identification of adipose tissue-derived EVs. (**A**) Schematic diagram of EVs isolated from adipose tissue collected from mice fed a chow or high-fat diet. Created in BioRender. Bao, X. (2025) https://BioRender.com/7ucfgo7. (**B**) Representative TEM images of CD-EVs and HFD-EVs. Scale bar: 200 nm. (**C**) The presence of marker proteins in CD-EVs and HFD-EVs. (**D**) PKH26-labeled CD-EVs and HFD-EVs were absorbed by AML12 cells. Scale bar: 50 μm.

AML12 cells for 6 h. Fluorescent staining experiments showed that PKH26-labelled EVs were detected in the perinuclear region of the cytoplasm of AML12 cells, indicating that CD-EVs and HFD-EVs were successfully internalized by hepatocytes (Figure 1D).

The Level of miR-141-3p in EVs Is Downregulated in Obese Environment

Our previous studies revealed that miR-141-3p as the primary small RNA mediating adipose tissue exosome-regulated insulin sensitivity.[29] The differential expressed levels of miR-141-3p in the CD-EVs and HFD-EVs were confirmed by qPCR. The results confirmed that the expression level of miR-141-3p was significantly decreased in the EVs secreted by the adipose tissue of HFD-fed mice (Figure 2A). Similarly, miR-141-3p levels in adipose tissue were significantly lower in the HFD group compared to the chow diet group (Figure 2B). Finally, we compared the levels of miR-141-3p in AML12 cells after treatment with EVs and found that the level of miR-141-3p in AML12 cells also increased with the addition of CD-EVs (Figure 2C). In addition, the melting curve and amplification efficiency of miR-141-3p are in Supplementary Figure 2.

https://doi.org/10.2147/IJN.S511842

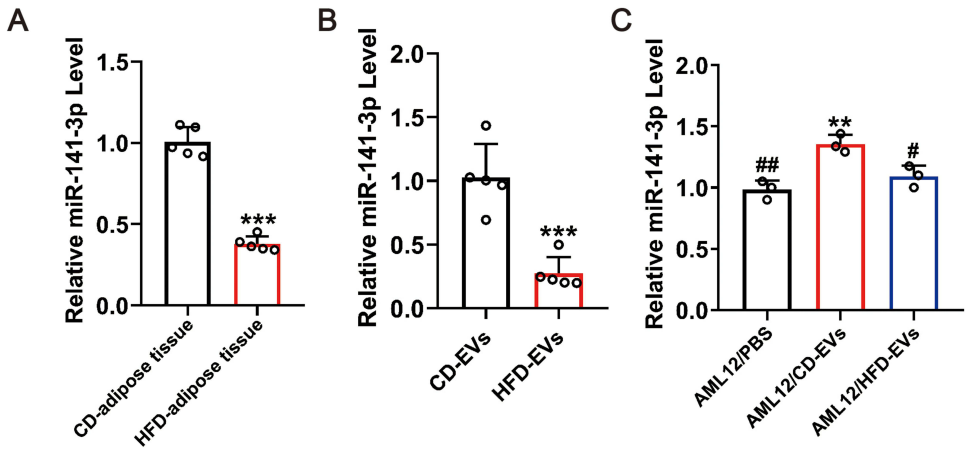

Figure 2 Detection of miR-141-3p expression levels in different samples. (**A**) Detection of miR-141-3p expression in the adipose tissue of obese and lean mice by qPCR. ***P< 0.001, HFD-adipose tissue vs CD-adipose tissue. n=5. (**B**) Comparison of miR-141-3p levels between HFD-EVs and CD-EVs. ***P<0.001, HFD-EVs vs CD-EVs. n=5. (**C**) The miR-141-3p level was detected by qPCR in AML12 cells with the administration of HFD-EVs, CD-EVs, or PBS. n=3. **P<0.01 compared to the PBS administration group, $^{\#}P$<0.05, $^{\#\#}P$<0.01 compared to the CD-EVs administration group. All values were expressed as mean ± SD.

Effects of miR-141-3p on Body Weight and Insulin Sensitivity in Mice

In previous work, we demonstrated that miR-141-3p mediates the functions of adipose tissue exosomes in hepatocytes, including significantly promoting insulin sensitivity and glucose uptake in vitro.[29] However, the role of miR-141-3p in vivo has not been explored. In this study, we sought to explore the effect of miR-141-3p in adipose tissue-derived EVs on obesity-induced insulin resistance in vivo. First, C57BL/6 male mice were fed a high-fat diet for 8 weeks. The body weight of the mice in the HFD group significantly increased (Supplementary Figure 1A). Interestingly, there was no significant difference in food intake among the mice (Supplementary Figure 1B). Moreover, glucose tolerance and insulin tolerance were impaired in the HFD group (Supplementary Figure 1C and D). These findings indicate that mice developed significant insulin resistance after being fed a high-fat diet for 8 weeks.

To investigate the role of miR-141-3p in insulin resistance, CD-EVs were first decorated with miR-141-3p inhibitor (CD-EVs-inhibitor) and inhibitor NC (CD-EVs-NC) followed by tail vein injection (Figure 3A). After CD-EVs transfection with the miR-141-3p inhibitor, miR-141-3p levels were reduced by nearly 64.33% compared with the CD-EVs-NC group (Figure 3B). However, the body weight and daily food intake had no obvious changes (Figure 3C and D). Furthermore, reducing the level of miR-141-3p in CD-EVs resulted in impaired glucose tolerance and insulin tolerance (Figure 3E and F). The HOMA-IR index more intuitively showed that the knockdown of miR-141-3p in CD-EVs reversed the effect of CD-EVs on improving insulin resistance (Figure 3G). These results indicate that miR-141-3p in CD-EVs can regulate insulin sensitivity.

To further confirm that miR-141-3p is the main molecule mediating EVs to regulate insulin sensitivity, we transfected miR-141-3p mimic or mimic NC into EVs to obtain HFD-EVs-mimics or HFD-EVs-NC (Figure 3H). Compared with the HFD-EVs-NC group, the level of miR-141-3p in the HFD-EVs-mimics group was increased by nearly 14.37 times (Figure 3I). The changes in body weight and food intake of the mice in each group were recorded every week, and there was no significant difference between the HFD-EVs-mimics and HFD-EVs-NC groups (Figure 3J and 3K). Compared with the HFD-EVs-NC group, mice treated with HFD-EVs-mimics showed higher glucose tolerance and insulin sensitivity (Figure 3L and M). The HOMA-IR index more intuitively confirmed that increasing the level of miR-141-3p in HFD-EVs improved insulin resistance (Figure 3N). Therefore, these results indicate that miR-141-3p is an important factor in mediating EVs to regulate insulin sensitivity in mice.

Effects of miR-141-3p in Adipose Tissue-Derived EVs on Hepatocyte Insulin Sensitivity

Given the prominent in vivo effects in regulating insulin sensitivity, we next investigated the in vitro function of miR-141-3p in hepatocytes. In contrast to previous work on normal hepatocytes,[29] we verified the effect on a hepatocyte model that mimics obesity-induced insulin resistance in vivo. First, AML12 cells were treated with sodium palmitate

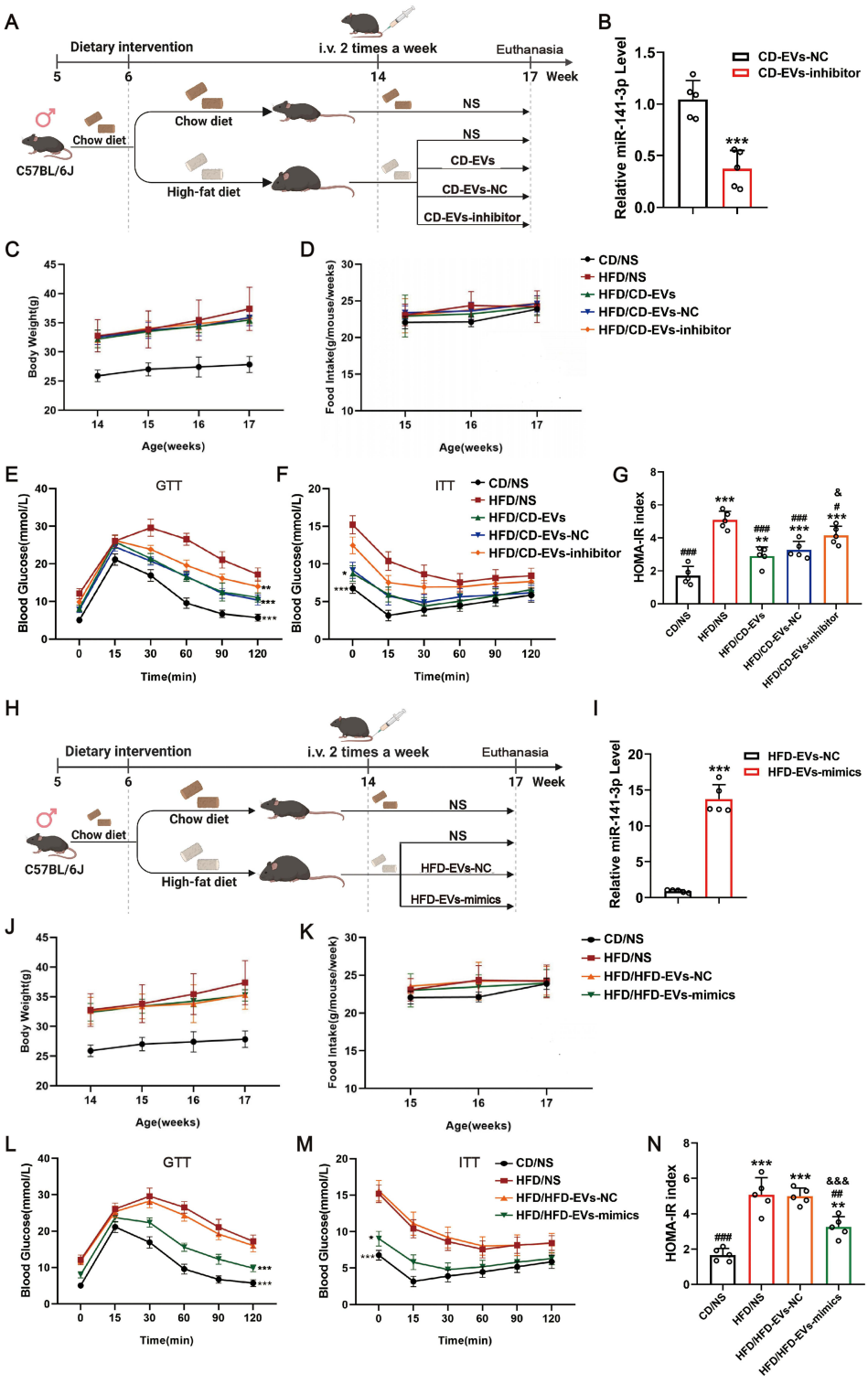

Figure 3 miR-141-3p in adipose tissue-derived EVs regulates obesity and insulin sensitivity in mice. (**A** and **H**) Schematic diagram of mouse model construction and different EVs interventions . (**A**) Created in BioRender. Bao, X. (2025) https://BioRender.com/czi6cco; (**H**) Created in BioRender. Bao, X. (2025) https://BioRender.com/0e8x5y1. (**B**) miR-141-3p levels in CD-EVs-NC and CD-EVs-inhibitor were detected by qPCR. ***P<0.001, the CD-EVs-inhibitor group vs the CD-EVs-NC group. (**C** and **D**) Body weight and weekly food intake of chow diet-fed mice and high-fat diet-fed mice administrated with CD-EVs, CD-EVs-NC, CD-EVs-inhibitor, or normal saline as indicated. (**E**–**G**) The GTT, ITT, and HOMA-IR index of mice were measured after administration for 3 weeks. HOMA-IR index = [fasting blood glucose levels (mmol/L)] × [fasting serum insulin levels (μU/mL)]/22.5. **P<0.01, ***P<0.001 compared to the CD/NS group. $^{\#}P$<0.05, $^{\#\#\#}P$<0.001 compared to the HFD/NS group. $^{\&}P$<0.05, the HFD/CD-EVs-inhibitor group vs the HFD/CD-EVs-NC group (**I**) miR-141-3p levels in HFD-EVs infected with miR-141-3p mimic or mimic NC were detected by qPCR. ***P<0.001, the HFD-EVs-mimics groups vs the HFD-EVs-NC group. (**J** and **K**) The body weight and weekly food intake of chow diet-fed mice and high-fat diet-fed mice administrated with HFD-EVs, HFD-EVs-NC, HFD-EVs-mimics, or normal saline. (**L**–**N**) The GTT, ITT, and HOMA-IR index of the mice in different treatment groups were measured. **P<0.01, ***P<0.001 compared to the CD/NS group. $^{\#}P$<0.05, $^{\#\#}P$<0.01, $^{\#\#\#}P$<0.001 compared to the HFD/NS group. $^{\&\&\&}P$<0.001, the HFD/HFD-EVs-mimics group vs the HFD/HFD-EVs-NC group. n=5. All values were expressed as mean ± SD.

https://doi.org/10.2147/IJN.S511842

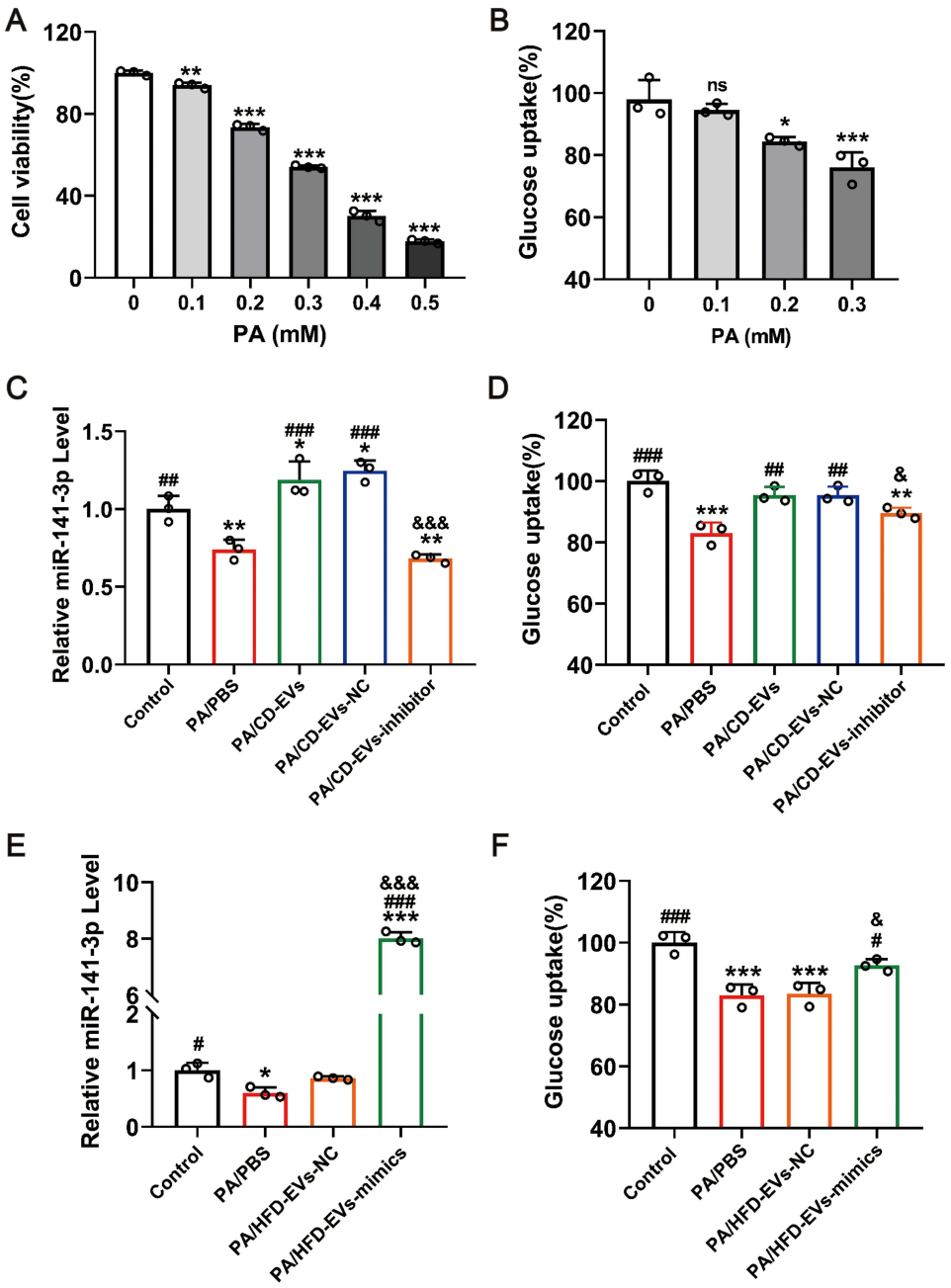

Figure 4 miR-141-3p in adipose tissue-derived EVs regulates insulin sensitivity in IR-AML12 cells. (**A**) Effects of PA on AML12 cell viability. (**B**) Effects on glucose uptake after treatment with PA for 24 h. **P*<0.05, ***P*<0.01, ****P*<0.001, different concentrations of PA group vs control group. (**C**) The levels of miR-141-3p in IR-AML12 cells after transfection of miR-141-3p inhibitor in CD-EVs. (**D**) Effects of glucose uptake in IR-AML12 cells after transfection of miR-141-3p inhibitor in CD-EVs. (**E**) The levels of miR-141-3p in different treatment groups were measured in cell after HFD-EVs were transfected with the miR-141-3p mimic. (**F**) Effects on glucose uptake in cell after transfection of the miR-141-3p mimic in HFD-EVs. **P*<0.05, ***P*<0.01, ****P*<0.001 compared to the Control group. $^{\#}P$<0.05, $^{\#\#}P$<0.01, $^{\#\#\#}P$<0.001 compared to the PA/PBS group. $^{\&}P$<0.05, $^{\&\&\&}P$<0.001, the PA/CD-EVs-inhibitor group vs the PA/CD-EVs-NC group or the PA/HFD-EVs-mimics group vs the PA/HFD-EVs-NC group. n=3. All values were expressed as mean ± SD.

(PA) for 24 h, which showed that PA reduced the survival and glucose uptake capacity in a dose-dependent manner (Figure 4A and B). At 0.3 mM PA, the cell survival rate was only approximately 50%, while 0.2 mM PA treatment significantly impaired glucose uptake compared to untreated controls. Therefore, 0.2 mM PA was used to construct an obesity-induced insulin resistance AML12 cells (IR-AML12) model. Compared with CD-EVs and CD-EVs-NC treatment groups, miR-141-3p expression was significantly reduced in IR-AML12 cells treated with the CD-EVs-inhibitor (Figure 4C). CD-EVs treatment significantly increased insulin-stimulated glucose uptake and AKT phosphorylation in

AML12 cells, while both glucose uptake and AKT phosphorylation in hepatocytes were inhibited by transfection with a miR-141-3p inhibitor (Figures 4D and 5C).

Next, we further explored the regulation of hepatocyte insulin sensitivity by miR-141-3p overexpression in HFD-EVs. First, we tested the levels of miR-141-3p in cells treated with HFD-EVs-mimics. The results showed that the levels of miR-141-3p in these cells were significantly elevated (Figure 4E). Furthermore, we evaluated the effects of miR-141-3p mimic modified HFD-EVs on cellular glucose uptake and AKT phosphorylation. Adipose tissue-derived EVs from obese mice significantly inhibited insulin-stimulated glucose uptake and AKT phosphorylation in AML12 cells, whereas HFD-EVs mimics treatment reversed this phenomenon (Figures 4F and 5D). These results indicate that miR-141-3p plays an important role in mediating EVs to regulate hepatic insulin sensitivity.

Effects of miR-141-3p in Adipose Tissue-Derived EVs on Hepatic Glycogen Synthesis and Gluconeogenesis in HFD Mice

Studies have shown that hepatic glycogen synthesis is decreased and hepatic gluconeogenesis is increased in type 2 diabetes.[4] This observation prompted us to evaluate whether miR-141-3p regulates insulin resistance by these pathways. As expected, liver glycogen content was reduced in the CD-EVs-inhibitor group compared with the CD-EVs-NC group, as indicated by liver tissue glycogen staining (Figure 6A). Glycogen content determination further indicated that the knockdown of miR-141-3p in CD-EVs reversed the promotion of liver glycogen synthesis by CD-EVs (Figure 6B). In addition, the expression levels of the gluconeogenic genes glucose-6-phosphatase (G6PC) and phosphoenolpyruvate carboxykinase (PCK) were elevated in the CD-EVs inhibitor group (Figure 6C and D). Western blotting results further showed that the knockdown of miR-141-3p in CD-EVs reversed the inhibition of liver G6PC and PCK protein expression by CD-EVs (Figure 6E). In addition, we further measured the effects of miR-141-3p overexpression in HFD-EVs on hepatic glycogen synthesis and gluconeogenesis in HFD mice. The miR-141-3p mimic transfection reversed the HFD-EVs-induced decrease in liver glycogen staining and content and the increase in gluconeogenic gene and protein expression (Figure 6F and G).

Effects of miR-141-3p in Adipose Tissue-Derived EVs on Glycogen Synthesis and Gluconeogenesis in Hepatocytes

Furthermore, we measured the influence of miR-141-3p knockdown in CD-EVs on insulin-stimulated cellular glycogen synthesis and gluconeogenesis. miR-141-3p knockdown significantly attenuated the promotive effect of CD-EVs on glycogen synthesis in AML12 cells, which was consistent with a decrease in glycogen concentration (Figure 7A and B). Moreover, infection of CD-EVs with the miR-141-3p inhibitor reversed the inhibitory effect of CD-EVs on the expression of gluconeogenic genes and proteins of G6PC and PCK (Figure 7C–E). In addition, glycogen staining results showed that HFD-EVs-mimics significantly promoted hepatocyte glycogen synthesis compared with the HFD-EVs-NC group (Figure 7F), as evidenced by glycogen content assays in hepatocytes (Figure 7G). Similarly, the expression of gluconeogenesis-related genes and proteins (G6PC and PCK) was also inhibited by HFD-EVs-mimics (Figure 7H–J). These data strongly suggest that miR-141-3p can mediate EVs to regulate insulin resistance in hepatocytes and hepatic tissue by regulating glycogen synthesis and gluconeogenesis.

miR-141-3p Regulates Hepatic Glycogen Synthesis and Gluconeogenesis by Activating the PI3K/AKT Signaling Pathway via PTEN

In the liver, AKT is a key regulator of insulin resistance, and its activation promotes glycogen synthesis while inhibiting gluconeogenesis.[34,35] Our previous experiments demonstrated miR-141-3p orchestrates PTEN, a critical modulator of insulin resistance in hepatocytes.[29] PTEN is reported to be upstream of the PI3K/AKT pathway,[36] so miR-141-3p may mediate insulin resistance through PTEN and the downstream PI3K/AKT pathway. To further prove our hypothesis, miR-141-3p inhibitor, inhibitor-NC, miR-141-3p mimic, or mimic-NC was transfected into CD-EVs or HFD-EVs, respectively. Western blotting analysis revealed that CD-EVs treatment significantly reduced PTEN expression, whereas miR-141-3p inhibition reversed this effect (Figure 5A). Similarly, overexpression of miR-141-3p in HFD-EVs markedly decreased PTEN protein levels compared to the PBS group, which conflicts with the results of HFD-EVs-NC treatment

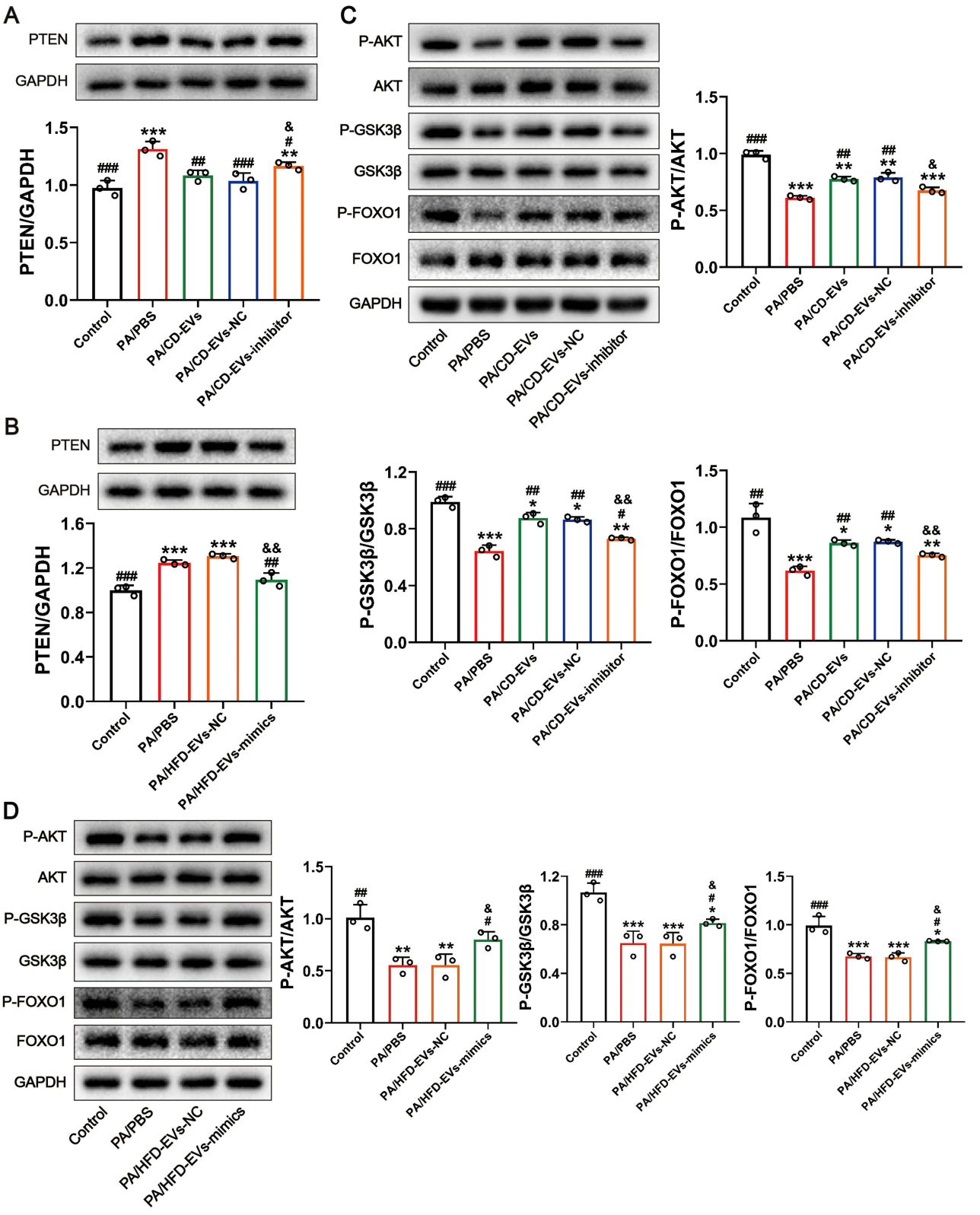

Figure 5 miR-141-3p regulates PI3K/AKT signaling in hepatocytes via PTEN. (**A**) Effect of CD-EVs transfected with the miR-141-3p inhibitor on PTEN protein expression. (**B**) Effect of HFD-EVs transfected with the miR-141-3p mimic on PTEN protein expression. (**C**) Effect of CD-EVs transfected with the miR-141-3p inhibitor on the phosphorylation of AKT, GSK3β and FOXO1. (**D**) Effect of HFD-EVs transfected with the miR-141-3p mimic on the phosphorylation of AKT, GSK3β and FOXO1. **P*<0.05, ***P*<0.01, ****P*<0.001 compared to the Control group. #*P*<0.05, ##*P*<0.01, ####*P*<0.001 compared to the PA/PBS group. &*P*<0.05, &&*P*<0.01, the PA/CD-EVs-inhibitor group vs the PA/CD-EVs-NC group or the PA/HFD-EVs-mimics group vs the PA/HFD-EVs-NC group. n=3. All values were expressed as mean ± SD.

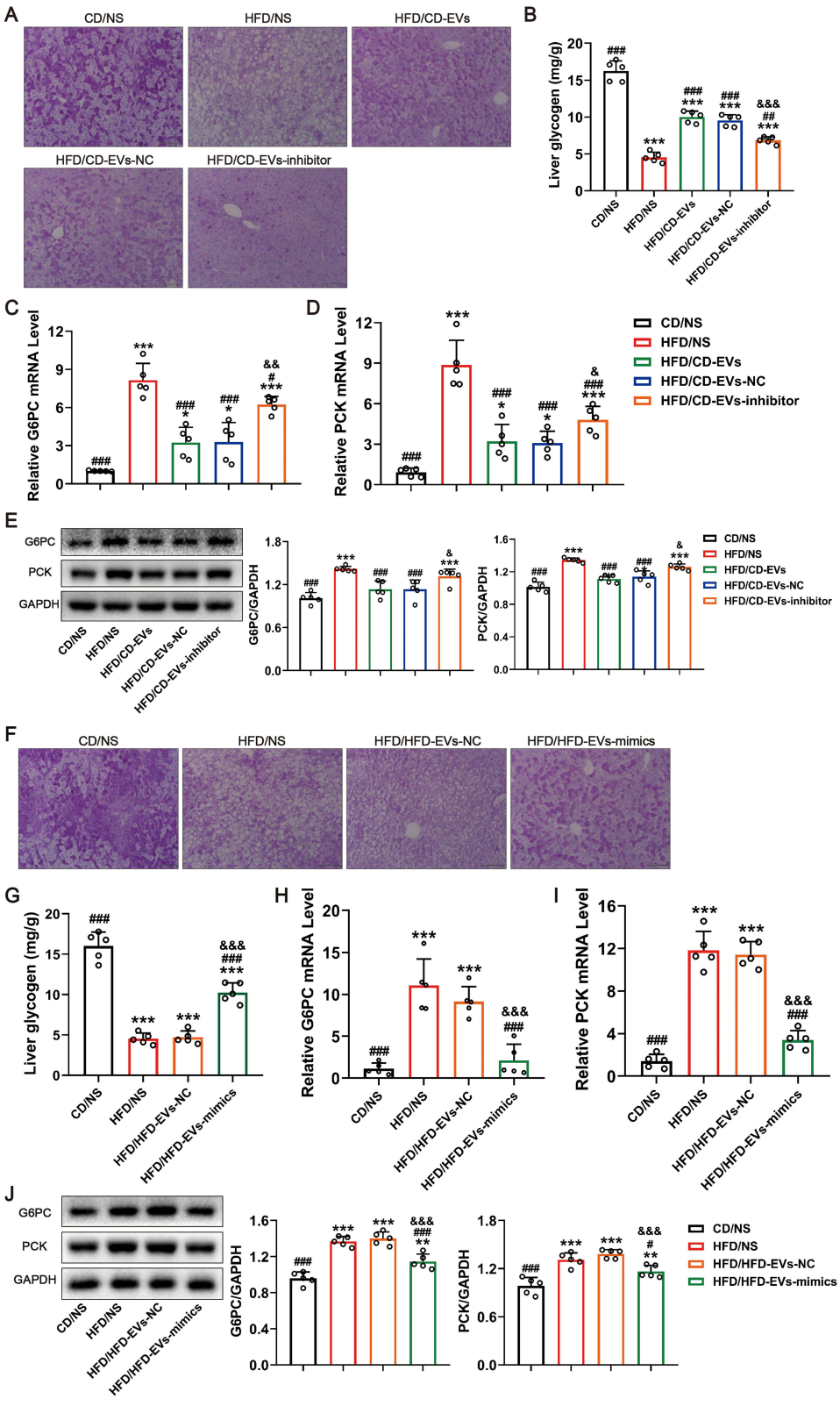

Figure 6 Adipose tissue-derived EVs regulate hepatic glycogen synthesis and gluconeogenesis through miR-141-3p. (**A** and **B**) PAS staining and liver glycogen content after transfection of CD-EVs with the miR-141-3p inhibitor. (**C** and **D**) qPCR analysis of G6PC and PCK expression in the liver after transfection of CD-EVs with the miR-141-3p inhibitor. (**E**) Western blotting of G6PC and PCK expression in the liver after transfection of CD-EVs with the miR-141-3p inhibitor. (**F** and **G**) PAS staining and liver glycogen content after transfection of HFD-EVs with the miR-141-3p mimic. (**H** and **I**) qPCR analysis of G6PC and PCK expression in the liver after transfection of HFD-EVs with the miR-141-3p mimic. (**J**) Western blotting of G6PC and PCK protein expression in the liver after transfection of HFD-EVs with the miR-141-3p mimic. **P*<0.05, ***P*<0.01, ****P*<0.001 compared to the CD/NS group. $^{\#}P$<0.05, $^{\#\#}P$<0.01, $^{\#\#\#}P$<0.001 compared to the HFD/NS group. $^{\&}P$<0.05, $^{\&\&}P$<0.01, $^{\&\&\&}P$<0.001, the HFD/CD-EVs-inhibitor group vs the HFD/CD-EVs-NC group or the HFD/HFD-EVs-mimics group vs the HFD/HFD-EVs-NC group. n=5. Scale bar: 100 μm. All values were expressed as mean ± SD.

https://doi.org/10.2147/IJN.S511842

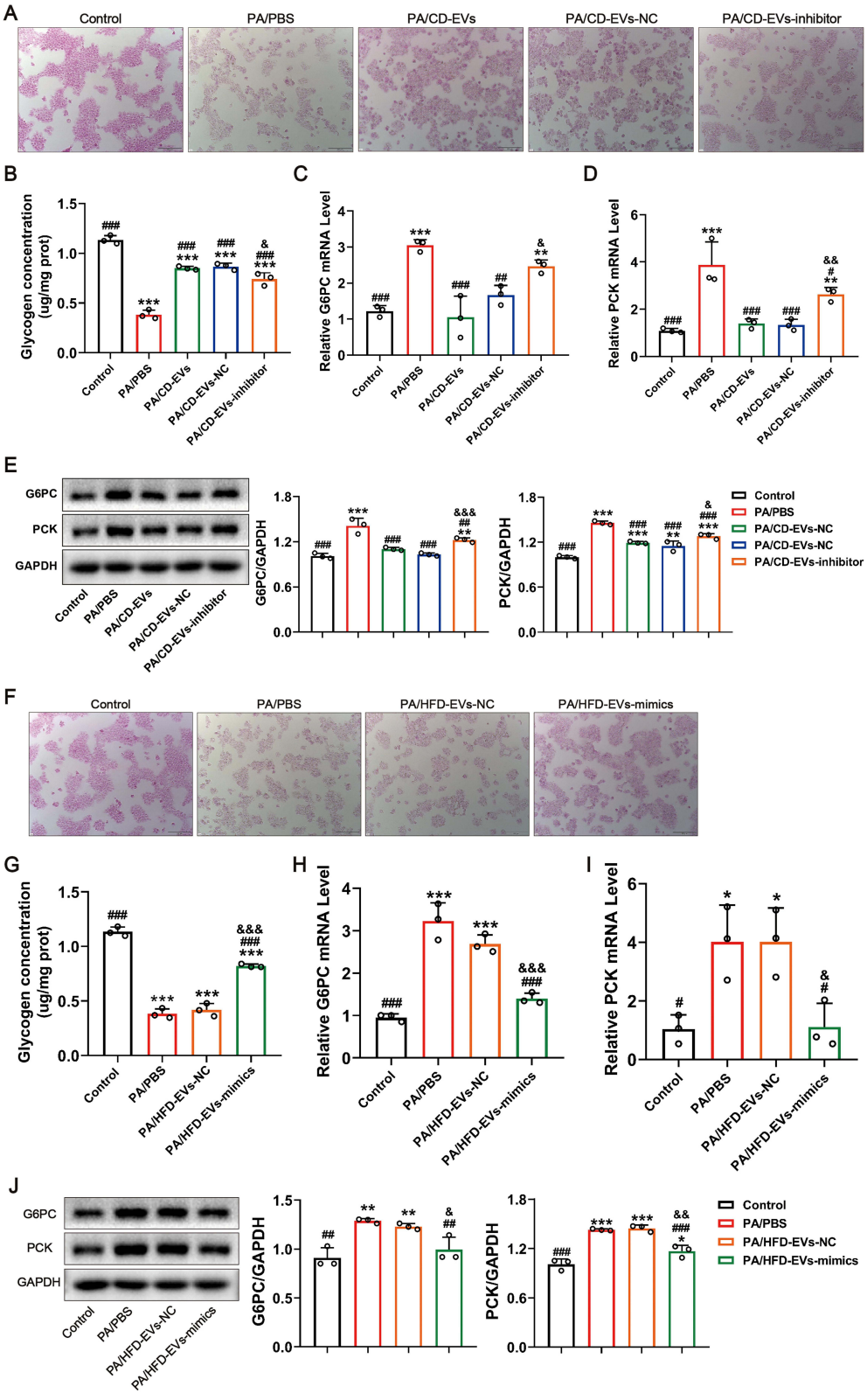

Figure 7 Effects of knocking down or overexpressing miR-141-3p in EVs on glycogen synthesis and gluconeogenesis in hepatocytes. (**A** and **B**) Effects of CD-EVs-inhibitor treatment on the PAS staining and glycogen content of hepatocytes. (**C** and **D**) Effects of CD-EVs-inhibitor treatment on G6PC and PCK mRNA expression. (**E**) Western blotting of G6PC and PCK protein expression after CD-EVs-inhibitor treatment of AML12 cells. (**F** and **G**) Effects of HFD-EVs-mimics treatment on the PAS staining and glycogen content of hepatocytes. (**H** and **I**) Effects of HFD-EVs-mimics treatment on G6PC and PCK mRNA expression. (**J**) Western blotting of G6PC and PCK protein expression after HFD-EVs-mimics treatment of AML12 cells. **P*<0.05, ***P*<0.01, ****P*<0.001 compared to the Control group. $^{\#}$*P*<0.05, $^{\#\#}$*P*<0.01, $^{\#\#\#}$*P*<0.001 compared to the PA/PBS group. $^{\&}$*P*<0.05, $^{\&\&}$*P*<0.01, $^{\&\&\&}$*P*<0.001, the PA/CD-EVs-inhibitor group vs the PA/CD-EVs-NC group or the PA/HFD-EVs-mimics group vs the PA/HFD-EVs-NC group. n=3. Scale bar: 200 μm. All values were expressed as mean ± SD.

(Figure 5B). Next, we investigated the effect of miR-141-3p on PI3K/AKT signaling. In hepatocytes, insulin-induced phosphorylation of Protein kinase B (AKT), Glycogen synthase kinase 3β (GSK3β), and Forkhead transcription factor 1 (FOXO1) was reduced after transfection with the miR-141-3p inhibitor compared with CD-EVs treatment, indicating impaired insulin signaling (Figure 5C). Furthermore, we measured the influence of overexpressing miR-141-3p in HFD-EVs on insulin signaling activation. In AML12 cells, miR-141-3p mimic transfection abrogated the PA-induced increase in AKT, GSK3β, and FOXO1 phosphorylation (Figure 5D). Collectively, these findings suggested that miR-141-3p is a positive regulatory factor of cellular insulin signaling. Furthermore, we measured the expression of PTEN in the liver of obese mice treated with CD-EVs-inhibitor and HFD-EVs-mimics. Transfection of CD-EVs with the miR-141-3p inhibitor significantly increased the protein level of PTEN (Figure 8A). In contrast, miR-141-3p overexpression in HFD-EVs significantly reduced the expression of PTEN (Figure 8B). We then studied the effect of miR-141-3p on insulin signaling in the mouse liver. Consistent with the results of the cell experiments, knockdown of miR-141-3p in CD-EVs significantly inhibited the CD-EVs-induced increase in the phosphorylation of the AKT, GSK3β and FOXO1 proteins in the liver (Figure 8C). In addition, HFD-EVs transfected with the miR-141-3p mimic significantly promoted the phosphorylation of the AKT, GSK3β and FOXO1 proteins in the liver (Figure 8D). Collectively, these findings indicate that miR-141-3p may mediate insulin resistance through PTEN and the downstream PI3K/AKT pathway.

Finally, we analyzed the expression of adipocyte-specific protein Adiponectin and macrophage-specific protein CD11b in EVs derived from adipose tissue, adipocytes, and macrophages using Western blotting. As shown in Supplementary Figure 3, Adiponectin was detected in both adipose tissue-derived EVs and 3T3-L1 cell-derived EVs, whereas CD11b remained nearly undetectable in adipose tissue-derived EVs.

Discussion

Obesity, as the primary driver of insulin resistance, constitutes a central mechanism in type 2 diabetes pathogenesis.[37] Emerging studies have confirmed the existence of close endocrine crosstalk between the liver and adipose tissue.[38] However, the molecular mechanisms of this interorgan communication remain to be elucidated. Notably, miRNAs in adipose tissue-derived EVs, acting as a novel class of endocrine factor, are closely related to liver-related diseases, including hepatic insulin resistance.[39,40] In the current study, we aimed to examine whether adipose tissue-derived EVs improve obesity-induced hepatic insulin resistance through miR-141-3p and delineate the underlying molecular mechanisms. As a member of the miR-200 family, miR-141-3p is widely implicated in cancer progression and metastasis.[29,41] Emerging evidence links miR-141-3p to insulin resistance and type 2 diabetes pathogenesis,[23] though its mechanistic role in metabolic disorders remains underexplored. In this study, we first confirmed that miR-141-3p was significantly downregulated in obesity-associated contexts, including the adipose tissue of obese mice, EVs derived from the adipose tissue of obese mice, and AML12 cells treated with HFD-EVs (Figure 2). This finding suggested that miR-141-3p may mediate adipose tissue-derived extracellular vesicle regulation of hepatic insulin resistance.

Hepatic insulin resistance is a key driver of type 2 diabetes. Recent studies have demonstrated that EVs derived from adipose tissue can improve insulin sensitivity by delivering functional miRNAs.[42] Given the pivotal role of hepatic glucose metabolism (including synthesis and breakdown) in systemic glucose homeostasis.[43] Identifying miRNAs that regulate this process is critical. This study focuses on miR-141-3p in adipose tissue-derived EVs, investigating its potential to alleviate insulin resistance through modulation of hepatic glucose metabolic pathways. In this study, we found that knockdown of miR-141-3p in CD-EVs resulted in impaired glucose tolerance and insulin tolerance, and reduced systemic insulin sensitivity in HFD-fed mice compared with those in CD-EVs-treated group (Figure 3A–G), whereas depletion of miR-141-3p in HFD-EVs significantly improved systemic insulin sensitivity (Figure 3H–N). Further in vivo and in vitro experiments revealed that CD-EVs-inhibitor treatment reversed the effects of CD-EVs on promoting glycogen synthesis and inhibiting gluconeogenesis, while HFD-EVs-mimics restored hepatic glucose metabolic balance (Figures 6 and 7). These findings collectively establish miR-141-3p as a central regulator of adipose tissue-derived EVs in ameliorating hepatic insulin resistance.

The inherent multi-target nature of miRNAs poses significant challenges in deciphering the regulatory mechanisms of specific miRNAs. This study focuses on PTEN, a core target of miR-141-3p, which acts as a critical negative regulator in the insulin signaling pathway. PTEN impairs hepatic insulin sensitivity by catalyzing PIP3 dephosphorylation, thereby suppressing PI3K/AKT signaling activation.[2,44,45] Our data demonstrate that miR-141-3p exerts its pivotal regulatory role

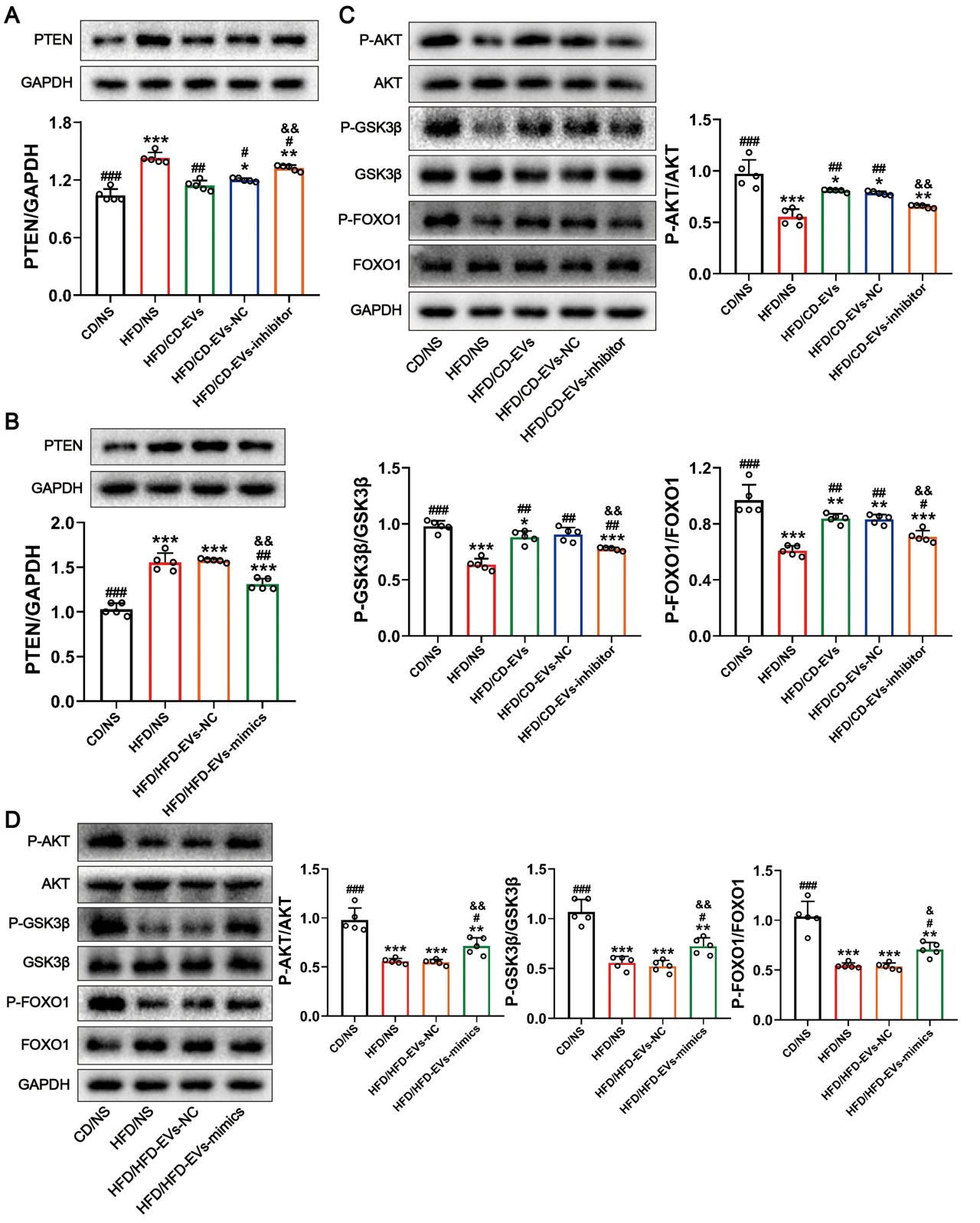

Figure 8 miR-141-3p regulates insulin signaling in the mouse liver via PTEN. (**A**) Effect of CD-EVs transfected with the miR-141-3p inhibitor on PTEN protein expression. (**B**) Effect of HFD-EVs transfected with the miR-141-3p mimic on PTEN protein expression. (**C**) Effect of CD-EVs transfected with miR-141-3p inhibitor on insulin signaling. (**D**) Effect of HFD-EVs transfected with the miR-141-3p mimic on insulin signaling. **P*<0.05, ***P*<0.01, ****P*<0.001 compared to the CD/NS group. $^{\#}$*P*<0.05, $^{\#\#}$*P*<0.01, $^{\#\#\#}$*P*<0.001 compared to the HFD/NS group. $^{\&}$*P*<0.05, $^{\&\&}$*P*<0.01, the HFD/CD-EVs-inhibitor group vs the HFD/CD-EVs-NC group or the HFD/HFD-EVs-mimics group vs the HFD/HFD-EVs-NC group. n=5. All values were expressed as mean ± SD.

in hepatic insulin signal transduction through direct targeting of PTEN. Knockdown of miR-141-3p in CD-EVs upregulated PTEN protein expression in hepatocytes and liver tissues while inhibiting phosphorylation of AKT, GSK3β, and FOXO1. Conversely, overexpression of miR-141-3p in HFD-EVs downregulated PTEN expression and concurrently activated phosphorylation of these proteins. These findings indicate that miR-141-3p enhances insulin signal transduction by targeting PTEN to alleviate its negative regulation of the PI3K/AKT pathway.

This study demonstrates that adipose tissue-derived EVs ameliorate obesity-associated hepatic insulin resistance via miR-141-3p-mediated PTEN inhibition and PI3K/AKT activation, redefining miR-141-3p as a metabolic regulator. Circulating EVs carrying miR-141-3p may serve as non-invasive biomarkers for early insulin resistance, while engineered EVs loaded with insulin-sensitizing molecules (eg, miR-141-3p or synergistic factors) hold promise as targeted therapeutic tools. However, this study has several limitations. First, the therapeutic potential of miR-141-3p-enriched EVs requires further validation in large animal models. Second, While the study primarily focused on hepatic glucose metabolism, the roles of miR-141-3p in lipid metabolism remains unclear. Additionally, we did not directly quantify the proportion of adipose tissue-derived EVs in circulating plasma or measure endogenous miR-141-3p levels in circulating EVs due to experimental constraints. Future investigations will employ tissue-specific EV tracking and multi-omics technologies to decipher systemic regulatory networks, ultimately advancing precision diagnostics and therapeutics for metabolic disorders.

Conclusion

In conclusion, our study is the first to reveal that EV-derived miR-141-3p from adipose tissue ameliorates obesity-induced hepatic insulin resistance by regulating hepatic glucose metabolism. This study unveils a novel paradigm in which obesity

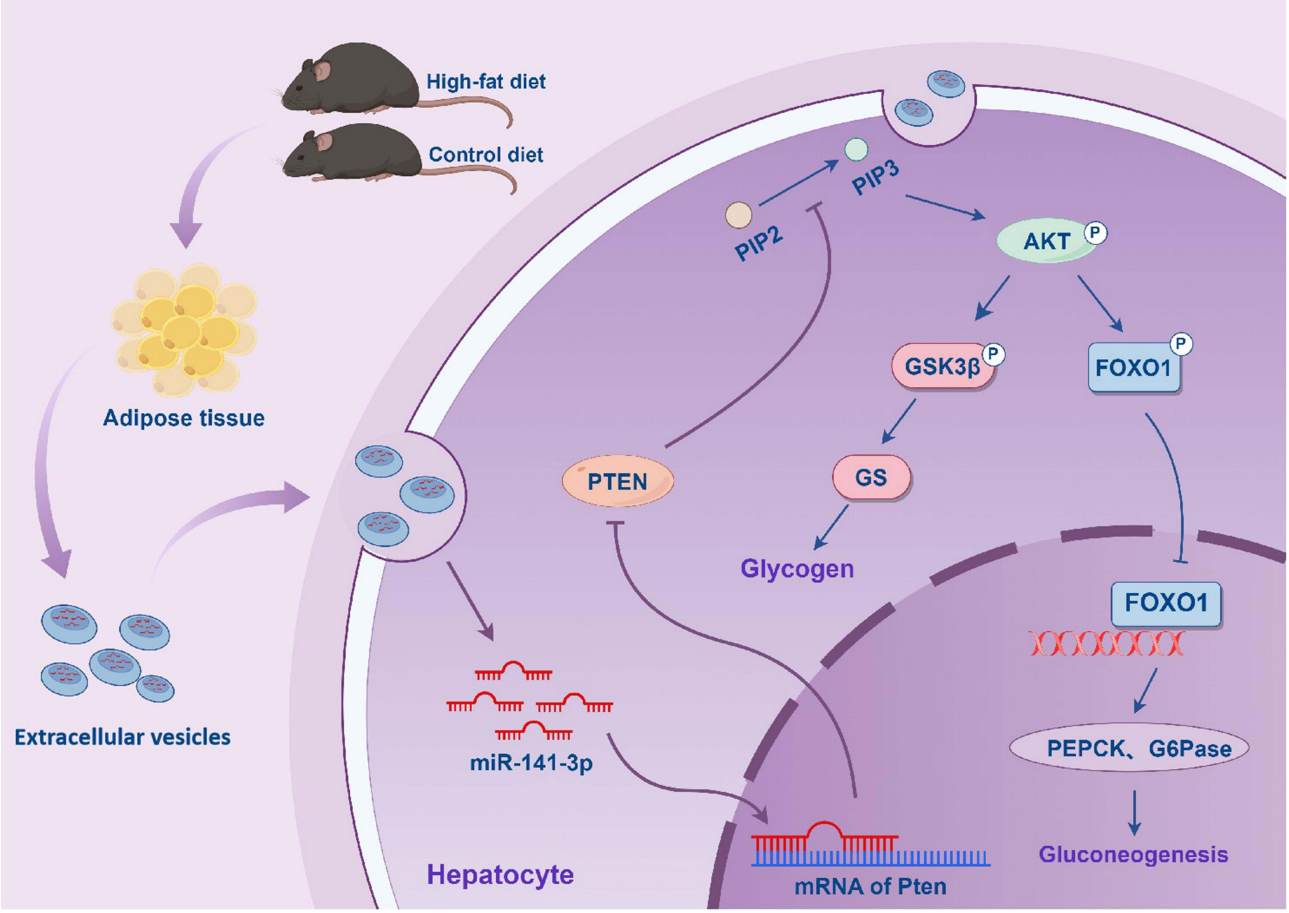

Figure 9 Schematic diagram of the mechanism revealed in this study. miR-141-3p regulates the expression of PTEN, further regulates the activation of the PI3K/AKT signaling pathway, and participates in the regulation of insulin resistance (By Figdraw).

https://doi.org/10.2147/IJN.S511842

reprograms miR-141-3p cargo within adipose tissue-derived EVs, enabling interorgan crosstalk to ameliorate hepatic insulin resistance. Mechanistically, adipose EV-derived miR-141-3p acts as a master regulator through PTEN targeting, dually coordinating hepatic glucose homeostasis by concurrently suppressing gluconeogenesis via the PI3K/AKT/FOXO1 axis and enhancing glycogen synthesis via the PI3K/AKT/GSK3β pathway-a previously unrecognized "single miRNA-dual pathway" strategy (Figure 9). Notably, miR-141-3p expression levels may serve as both a therapeutic target and early diagnostic biomarker for metabolic disorders. These findings not only highlight miR-141-3p's dual role in combating insulin resistance and type 2 diabetes mellitus, but also redefine the role of adipose tissue-derived EVs in systemic metabolic regulation and open promising avenues for diagnosing and treating insulin resistance-related disorders.

Abbreviations

T2D, Type 2 diabetes; IR, Insulin resistance; EVs, Extracellular vesicles; PTEN, Phosphatase and tensin homolog; FGF, Fibroblast growth factor; IGF, Insulin-like growth factor; TNF-α, Tumor necrosis factor α; IL-6, Interleukin 6; miRNA, microRNA; FBS, Fetal bovine serum; ITS, Insulin–Transferrin–Selenium Solution; 3'UTR, 3'untranslated region; CD, Chow diet; HFD, High-fat diet; CD-EVs, Adipose tissue-derived extracellular vesicles from mice fed with the chow diet; HFD-EVs, Adipose tissue-derived extracellular vesicles from mice fed with a high-fat diet; CD-EVs-NC, CD-EVs treated with microRNA inhibitor N.C; CD-EVs-inhibitor, CD-EVs treated with miR-141-3p inhibitor; HFD-EVs-NC, HFD-EVs treated with microRNA Negative Control; HFD-EVs-mimics, HFD-EVs treated with miR-141-3p mimic; PIP3, Phosphorylated inositol triphosphate; PI3K, Phosphatidyl-inositol 3-kinase; AKT, Protein kinase B; G6PC, Glucose 6 phosphate kinase; PCK, Phosphoenolpyruvate carboxykinase; FOXO1, Forkhead transcription factor 1; GSK3β, Glycogen synthase kinase 3β; GAPDH, Glyceraldehyde 3-phosphate dehydrogenase; HGP, Hepatic glucose production; P-AKT, Phosphorylated AKT; P-FOXO1, Phosphorylated FOXO1; P-GSK3β, Phosphorylated GSK3β; GTT, Glucose tolerance test; ITT, Insulin tolerance test; PAS, Periodic acid-Schiff; NS, Normal saline.

Ethics Approval and Informed Consent

All animal experiments were carried out according to the Guidelines for the Care and Use of Laboratory Animals of the Chinese Animal Welfare Committee and protocols were approved by the Animal Care Committee of Jinan University (approval number: IACUC-20190827-03).

Author Contributions

All authors made a significant contribution to the work reported, whether that is in the conception, study design, execution, acquisition of data, analysis and interpretation, or in all these areas; took part in drafting, revising or critically reviewing the article; gave final approval of the version to be published; have agreed on the journal to which the article has been submitted; and agree to be accountable for all aspects of the work.

Funding

This study was financially supported by the National Natural Science Foundation of China (No. 82373773 and 82400714), the Guangdong Basic and Applied Basic Research Foundation (No. 2024A1515012921), the Guangdong S&T Program (No. 2024B1111160006 and 2022B1111070007).

Disclosure

The authors report no conflicts of interest in this work.

References

1. Lee SH, Park SY, Choi CS. Insulin resistance: from mechanisms to therapeutic strategies. *Diabetes Metab J*. 2022;46(1):15–37. doi:10.4093/dmj.2021.0280
2. Santoleri D, Titchenell PM. Resolving the paradox of hepatic insulin resistance. *Cell Mol Gastroenterol Hepatol*. 2019;7(2):447–456. doi:10.1016/j.jcmgh.2018.10.016
3. Titchenell PM, Lazar MA, Birnbaum MJ. Unraveling the regulation of hepatic metabolism by insulin. *Trends Endocrinol Metab*. 2017;28(7):497–505. doi:10.1016/j.tem.2017.03.003

4. Liu TY, Shi CX, Gao R, et al. Irisin inhibits hepatic gluconeogenesis and increases glycogen synthesis via the PI3K/Akt pathway in type 2 diabetic mice and hepatocytes. *Clin Sci*. 2015;129(10):839–850. doi:10.1042/cs20150009
5. Samuel VT, Shulman GI. Mechanisms for insulin resistance: common threads and missing links. *Cell*. 2012;148(5):852–871. doi:10.1016/j.cell.2012.02.017
6. Johnson AM, Olefsky JM. The origins and drivers of insulin resistance. *Cell*. 2013;152(4):673–684. doi:10.1016/j.cell.2013.01.041
7. Klein S, Gastaldelli A, Yki-Järvinen H, Scherer PE. Why does obesity cause diabetes? *Cell Metab*. 2022;34(1):11–20. doi:10.1016/j.cmet.2021.12.012
8. Taylor R, Al-Mrabeh A, Sattar N. Understanding the mechanisms of reversal of type 2 diabetes. *Lancet Diabetes Endocrinol*. 2019;7(9):726–736. doi:10.1016/s2213-8587(19)30076-2
9. Flippo KH, Potthoff MJ. Metabolic messengers: FGF21. *Nat Metab*. 2021;3(3):309–317. doi:10.1038/s42255-021-00354-2
10. Ohlsson C, Mohan S, Sjögren K, et al. The role of liver-derived insulin-like growth factor-I. *Endocr Rev*. 2009;30(5):494–535. doi:10.1210/er.2009-0010
11. Wu J, Dong T, Chen T, et al. Hepatic exosome-derived miR-130a-3p attenuates glucose intolerance via suppressing PHLPP2 gene in adipocyte. *Metabolism*. 2020;103:154006. doi:10.1016/j.metabol.2019.154006
12. Cao H. Adipocytokines in obesity and metabolic disease. *J Endocrinol*. 2014;220(2):T47–59. doi:10.1530/joe-13-0339
13. Romacho T, Elsen M, Röhrborn D, Eckel J. Adipose tissue and its role in organ crosstalk. *Acta Physiol*. 2014;210(4):733–753. doi:10.1111/apha.12246
14. Isaac R, Reis FCG, Ying W, Olefsky JM. Exosomes as mediators of intercellular crosstalk in metabolism. *Cell Metab*. 2021;33(9):1744–1762. doi:10.1016/j.cmet.2021.08.006
15. Qin M, Xing L, Wu J, et al. Skeletal muscle-derived exosomal miR-146a-5p inhibits adipogenesis by mediating muscle-fat axis and targeting GDF5-PPARγ signaling. *Int J Mol Sci*. 2023;24(5):4561. doi:10.3390/ijms24054561
16. O'Brien K, Breyne K, Ughetto S, Laurent LC, Breakefield XO. RNA delivery by extracellular vesicles in mammalian cells and its applications. *Nat Rev Mol Cell Biol*. 2020;21(10):585–606. doi:10.1038/s41580-020-0251-y
17. Mathieu M, Martin-Jaular L, Lavieu G, Théry C. Specificities of secretion and uptake of exosomes and other extracellular vesicles for cell-to-cell communication. *Nat Cell Biol*. 2019;21(1):9–17. doi:10.1038/s41556-018-0250-9
18. Castaño C, Kalko S, Novials A, Párrizas M. Obesity-associated exosomal miRNAs modulate glucose and lipid metabolism in mice. *Proc Natl Acad Sci U S A*. 2018;115(48):12158–12163. doi:10.1073/pnas.1808855115
19. Zhou X, Li Z, Qi M, et al. Brown adipose tissue-derived exosomes mitigate the metabolic syndrome in high fat diet mice. *Theranostics*. 2020;10(18):8197–8210. doi:10.7150/thno.43968
20. Agbu P, Carthew RW. MicroRNA-mediated regulation of glucose and lipid metabolism. *Nat Rev Mol Cell Biol*. 2021;22(6):425–438. doi:10.1038/s41580-021-00354-w
21. Mo Y, Leung LL, Mak CSL, et al. Tumor-secreted exosomal miR-141 activates tumor-stroma interactions and controls premetastatic niche formation in ovarian cancer metastasis. *Mol Cancer*. 2023;22(1):4. doi:10.1186/s12943-022-01703-9
22. Huang S, Wa Q, Pan J, et al. Downregulation of miR-141-3p promotes bone metastasis via activating NF-κB signaling in prostate cancer. *J Exp Clin Cancer Res*. 2017;36(1):173. doi:10.1186/s13046-017-0645-7
23. Doumatey AP, Xu H, Huang H, et al. Global gene expression profiling in omental adipose tissue of morbidly obese diabetic African Americans. *J Endocrinol Metab*. 2015;5(3):199–210. doi:10.14740/jem286w
24. Li XY, Wang SS, Han Z, et al. Triptolide restores autophagy to alleviate diabetic renal fibrosis through the miR-141-3p/PTEN/Akt/mTOR pathway. *Mol Ther Nucleic Acids*. 2017;9:48–56. doi:10.1016/j.omtn.2017.08.011
25. Ji J, Qin Y, Ren J, et al. Mitochondria-related miR-141-3p contributes to mitochondrial dysfunction in HFD-induced obesity by inhibiting PTEN. *Sci Rep*. 2015;5(1):16262. doi:10.1038/srep16262
26. Li YZ, Di Cristofano A, Woo M. Metabolic role of PTEN in insulin signaling and resistance. *Cold Spring Harb Perspect Med*. 2020;10(8):a036137. doi:10.1101/cshperspect.a036137
27. Manna P, Jain SK. Phosphatidylinositol-3,4,5-triphosphate and cellular signaling: implications for obesity and diabetes. *Cell Physiol Biochem*. 2015;35(4):1253–1275. doi:10.1159/000373949
28. Grinder-Hansen L, Ribel-Madsen R, Wojtaszewski JF, Poulsen P, Grunnet LG, Vaag A. A common variation of the PTEN gene is associated with peripheral insulin resistance. *Diabetes Metab*. 2016;42(4):280–284. doi:10.1016/j.diabet.2016.03.003
29. Dang SY, Leng Y, Wang ZX, et al. Exosomal transfer of obesity adipose tissue for decreased miR-141-3p mediate insulin resistance of hepatocytes. *Int J Biol Sci*. 2019;15(2):351–368. doi:10.7150/ijbs.28522
30. Li X, Qin Y, Yue F, Lü X. Comprehensive analysis of fecal microbiome and metabolomics uncovered dl-norvaline-ameliorated obesity-associated disorders in high-fat diet-fed obese mice by targeting the gut microbiota. *J Agric Food Chem*. 2025;73(4):2381–2392. doi:10.1021/acs.jafc.4c06638
31. Wang Y, Li M, Chen L, et al. Natural killer cell-derived exosomal miR-1249-3p attenuates insulin resistance and inflammation in mouse models of type 2 diabetes. *Signal Transduct Target Ther*. 2021;6(1):409. doi:10.1038/s41392-021-00805-y
32. Ying W, Riopel M, Bandyopadhyay G, et al. Adipose tissue macrophage-derived exosomal miRNAs can modulate in vivo and in vitro insulin sensitivity. *Cell*. 2017;171(2):372–384e312. doi:10.1016/j.cell.2017.08.035
33. Xu L, Li Y, Yin L, et al. miR-125a-5p ameliorates hepatic glycolipid metabolism disorder in type 2 diabetes mellitus through targeting of STAT3. *Theranostics*. 2018;8(20):5593–5609. doi:10.7150/thno.27425
34. Huang X, Liu G, Guo J, Su Z. The PI3K/AKT pathway in obesity and type 2 diabetes. *Int J Biol Sci*. 2018;14(11):1483–1496. doi:10.7150/ijbs.27173
35. Ren Z, Xie Z, Cao D, et al. C-Phycocyanin inhibits hepatic gluconeogenesis and increases glycogen synthesis via activating Akt and AMPK in insulin resistance hepatocytes. *Food Funct*. 2018;9(5):2829–2839. doi:10.1039/c8fo00257f
36. Haddadi N, Lin Y, Travis G, Simpson AM, Nassif NT, McGowan EM. PTEN/PTENP1: 'regulating the regulator of RTK-dependent PI3K/Akt signalling', new targets for cancer therapy. *Mol Cancer*. 2018;17(1):37. doi:10.1186/s12943-018-0803-3
37. Ruze R, Liu T, Zou X, et al. Obesity and type 2 diabetes mellitus: connections in epidemiology, pathogenesis, and treatments. *Front Endocrinol*. 2023;14:1161521. doi:10.3389/fendo.2023.1161521

38. Sun W, Nie T, Li K, et al. Hepatic CPT1A facilitates liver-adipose cross-talk via induction of FGF21 in mice. *Diabetes*. 2021. doi:10.2337/db21-0363
39. Vienberg S, Geiger J, Madsen S, Dalgaard LT. MicroRNAs in metabolism. *Acta Physiol*. 2017;219(2):346–361. doi:10.1111/apha.12681
40. Peng C, Wang YL. Editorial: microRNAs as new players in endocrinology. *Front Endocrinol*. 2018;9:459. doi:10.3389/fendo.2018.00459
41. Ye Y, Li SL, Ma YY, et al. Exosomal miR-141-3p regulates osteoblast activity to promote the osteoblastic metastasis of prostate cancer. *Oncotarget*. 2017;8(55):94834–94849. doi:10.18632/oncotarget.22014
42. Liu T, Sun YC, Cheng P, Shao HG. Adipose tissue macrophage-derived exosomal miR-29a regulates obesity-associated insulin resistance. *Biochem Biophys Res Commun*. 2019;515(2):352–358. doi:10.1016/j.bbrc.2019.05.113
43. Han HS, Kang G, Kim JS, Choi BH, Koo SH. Regulation of glucose metabolism from a liver-centric perspective. *Exp Mol Med*. 2016;48(3):e218. doi:10.1038/emm.2015.122
44. Li A, Qiu M, Zhou H, Wang T, Guo W. PTEN insulin resistance and cancer. *Curr Pharm Des*. 2017;23(25):3667–3676. doi:10.2174/1381612823666170704124611
45. Guo S. Molecular basis of insulin resistance: the role of irs and foxo1 in the control of diabetes mellitus and its complications. *Drug Discov Today Dis Mech*. 2013;10(1–2):e27–e33. doi:10.1016/j.ddmec.2013.06.003